

Region-filtering Correlation Tracking

Nana Fan, Zhenyu He

Harbin Institute of Technology

Abstract. Recently, correlation filters have demonstrated the excellent performance in visual tracking. However, the base training sample region is larger than the object region, including the Interference Region (IR). The IRs in training samples from cyclic shifts of the base training sample severely degrade the quality of a tracking model. In this paper, we propose the novel Region-filtering Correlation Tracking (RFCT) to address this problem. We immediately filter training samples by introducing a spatial map into the standard CF formulation. Compared with existing correlation filter trackers, our proposed tracker has the following advantages: (1) The correlation filter can be learned on a larger search region without the interference of the IR by a spatial map. (2) Due to processing training samples by a spatial map, it is more general way to control background information and target information in training samples. The values of the spatial map are not restricted, then a better spatial map can be explored. (3) The weight proportions of accurate filters are increased to alleviate model corruption. Experiments are performed on two benchmark datasets: OTB-2013 and OTB-2015. Quantitative evaluations on these benchmarks demonstrate that the proposed RFCT algorithm performs favorably against several state-of-the-art methods.

Keywords: Visual Tracking, Correlation Filter

1 Introduction

Visual tracking is a fundamental problem in computer vision. Given the position of an object in the first frame, visual tracking aims to sequentially locate the object in the rest of an image sequence. Although many algorithms have been proposed in the recent years, visual tracking is still a challenge as a result of complex scenes.

In recent years, correlation filter based methods [1,2,3,4] have shown notable performance in standard benchmarks, partly because of their efficiency in exploiting more training samples. The correlation filter is introduced by Bolme *et al.* [5] into visual tracking, correlated over an exemplar to gain a desired Gaussian response. It is time-consuming to immediately derive the correlation filter from least square loss in the time domain. Therefore, to create a fast tracker, the correlation operation is transformed to the Fourier domain by Convolution Theorem. Then, the correlation filter can be solved by the efficiently element-wise operation. KCF [6] explains the correlation filter by means of generally known ridge regression and derives a new kernelized correlation filter. In this way, the correlation is reformulated as that the circulant matrix, which denotes all training samples from circulating shift of a base training sample, multiplies by the filter. It provides a deeper understanding for the correlation filter. And the result is the same as that in [5]. Correlation filter trackers have achieved state-of-the-art performances, but they still have a problem in the training procedure.

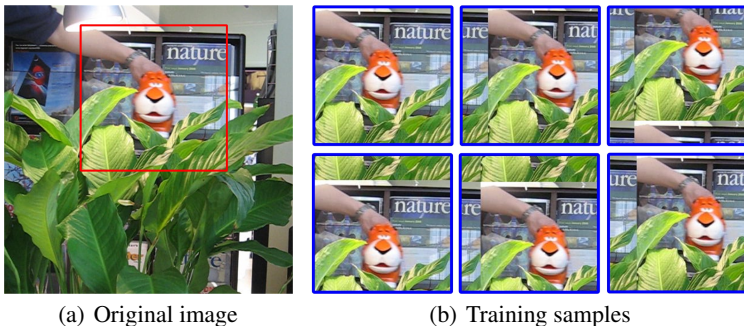


Fig. 1. (a) An original image and a base training sample. (b) Some training samples are from cyclic shifts of the base training sample. The base training sample region is larger than the object region, including the IR. It leads to that training samples contains IRs, which severely degrade the tracking quality.

Problem in Training Procedure: When the correlation filter is introduced into visual tracking, it needs to fit the tracking task. Generally, to detect the object by one correlation operation in the next frame, the base training sample region is larger than the target region (see Fig. 1(a)). Training samples are from cyclic shifts [6] of the base training sample (see Fig. 1(b)). By the Convolution Theorem, the correlation in the time domain corresponds to an element-wise multiplication in the Fourier domain. Therefore, the filter has the same size as the training samples. Obviously, the filter is not modeled for the object, but modeled for the object and its background in the base training sample. We name the background region Interference Region (IR). The IRs in training samples severely degrade the tracking quality. This is the challenge that this paper addresses.

To deal with the above problem, SRDCF [7] introduces a regularization component to penalize correlation filter coefficients depending on the corresponding spatial location. But, it only can penalize the correlation filter coefficients which are far away from the center. When a search region is very large, the edge coefficients of the filter should not works. Different to CFBL [8] and BACF [3], we model a filter for the base training sample, then exploit a spatial map to process the training samples. It is a more general way to control background information and target information within the training samples.

Contribution: In this paper, we propose Region-filtering Correlation Tracking (RFCT). The contributions of this work are summarized as follows.

- We model a filter for the base training sample and introduce a spatial map into the standard CF formulation for processing all the training samples. Compared with the correlation filter trackers, it is a more general way to control background information and target information in training samples. The values of the spatial map are not restricted, then a better spatial map can be explored.

- We increase the weight proportions of accurate filters for model update to alleviate model corruption.

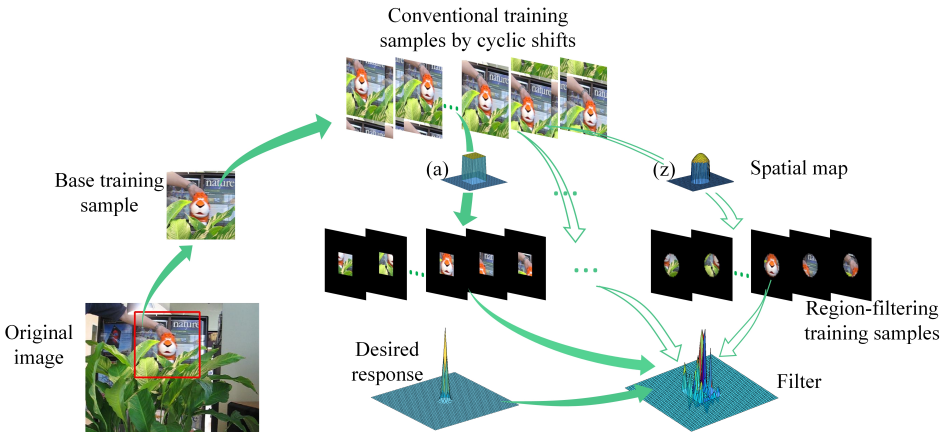


Fig. 2. Filtering the IRs. After locating the target, a base training sample is extracted, centered at the target. Training samples are from cyclic shifts of the base training sample. Because the base training sample region is larger than the target region, there are the IRs in training samples. The IRs severely degrade the quality of the tracking algorithm. In our approach, a spatial map is used to filter training samples. The values of the spatial map are not restricted. For example, when a binary map (a) is used, it can eliminate the influence of the IR. Or when a map (z) is used, it can eliminate the influence of the IR and penalize the edge of the target region.

2 Related Work

In visual tracking, the correlation filter has attracted wide attention, partly due to efficiently exploiting more training samples. Bolme *et al.* [5] firstly introduce correlation filter into visual tracking with grayscale samples, keeping the object scale fixed in tracking. Afterwards, some methods [9,10,11,6,12,13] improve performance with the help of multi-channel features, such as HOG [14] or Color-Names [15]. KCF [6] and MKCF [13] make kernelized extensions of linear correlation filter to further improve the performance. On the basic of multi-channel features, DSST [16] learns a correlation filter on a scale pyramid representation to catch the accurate object scale at real-time frame-rates. In term of the desired response, Bibi *et al.* [17] offset the effect of using scores of circularly shifted samples, replacing the hand-crafted Gaussian response by an adaptive response with scores of actual translations. Different from the traditional square loss, Wang *et al.* [18] draw lessons from the structured output tracker [19] to learn a correlation filter in a large-margin framework. The other method [20] proposes three sparse-based loss functions, and reveals the sensitivity of the peak values of the filter

in successive frames is consistent with the tracking performance from an experimental perspective. To deal with partial occlusion, some researchers [21,22,23] have proposed to introduce the part-based strategy into correlation filter tracking. SCF [21] limits all individual parts to keep close to each other for preserving the target object structure. The two works [22,23] apply an individual correlation filter for each part and rely on more reliable parts to locate the object. In addition, there are also some methods [24,25] with the aid of circulant matrix used in correlation filters to make the trackers run faster. Zuo *et al.* [24] reformulate the SVM model with circulant matrix expression and present an efficient alternating optimization method. CST [25] introduces the circulant structure property into a sparse tracker to reduce particles and be solved efficiently.

In correlation filter tracking, a search region is larger than the target region. Therefore, the base training sample not only covers the target, but also contains the IR. Because training samples are from cyclic shifts of the base training sample, the IRs in the training samples degrade the tracking quality. To deal with the above problem, some works [7,26,8,3] have made successful attempts. Different to them, we model a filter for a base training sample and exploit a spatial map to process all the training samples. The values of the spatial map are not restricted, examples of the spatial map are shown in Fig. 2. It is a general way to control background information and target information in the training samples.

2.1 Standard Correlation Filter Tracking

The aim of CF is to learn a correlation filter from a base training sample x with d channels. We indicate feature channel $l \in \{1, \dots, d\}$ of x by x_l . All training samples from cyclic shifts of the base training sample have the same spatial size $M \times N$. Then there is a training sample $x(m, n)$ at each spatial location $(m, n) \in \Omega := \{0, \dots, M-1\} \times \{0, \dots, N-1\}$. The desired response y is a scalar function over Ω , including a label for each location. CF can be formulated in the spatial domain as a ridge regression,

$$\min_{w_l} \sum_{l=1}^d \|X_l^\top w_l - y\|^2 + \lambda \|w_l\|^2, \quad (1)$$

where X_l is the circulant matrix of the base training sample x in the l -th channel, \top denotes the transpose, y is the desired response, λ is a regularization parameter that controls overfitting and w_l is the l -th channel of the filter w with the same size as the base training sample x . Moreover, it can also be expressed by the convolution operation,

$$\min_{w_l} \sum_{l=1}^d \|x_l * w_l - y\|^2 + \lambda \|w_l\|^2. \quad (2)$$

Here, $*$ denotes circular convolution. By Parseval's formula, Eq.2 can be transformed to the Fourier domain where the correlation filter is obtained by the element-wise operation.

Similar to the training stage, a test sample z is used for detection by the convolution operation. The scores S in the search region to which the test sample corresponds can

be computed by the inverse Discrete Fourier Transform (DFT),

$$S(z) = \mathcal{F}^{-1} \left(\sum_{l=1}^d \hat{z}_l \odot \hat{w}_l \right), \quad (3)$$

where \odot indicates element-wise product, $\hat{\cdot}$ is the DFT and \mathcal{F}^{-1} denotes the inverse DFT. Generally, the location with the maximum in the search region is regarded as the tracking result.

3 Region-filtering Correlation Tracking

In this section, we give a detailed description of our proposed method. Firstly, we introduce the problem formulation. Secondly, we derive the optimization algorithm. Thirdly, we analyse the model update strategy. Fourthly, we summarize the tracking framework.

3.1 Problem Formulation

Focusing on the challenge presented above, we exploit a spatial map to filter training samples, visualized in Fig.2. A spatial map is based on a priori information about the object location in the base training sample. And the spatial map can be any type, it can be a binary map eliminating the influence of the IRs, or a map similar to Gaussian penalizing the IRs, and so on. The spatial map c with the size $M \times N$ is embedded into the standard CF formulation Eq.1,

$$\min_{w_l} \sum_{l=1}^d \|X_l^\top \text{diag}(c)w_l - y\|_2^2 + \lambda \|w_l\|_2^2, \quad (4)$$

where $\text{diag}(c)$ is the diagonal matrix with the elements of the vector c in its diagonal. To solve Eq.4, we involve the introduction of an auxiliary variable t . In this case, Eq.4 can be identically reformulated as,

$$\begin{aligned} \min_{w_l, t_l} \sum_{l=1}^d \|X_l^\top t_l - y\|_2^2 + \lambda \|w_l\|_2^2 \\ \text{s.t. } t_l = \text{diag}(c)w_l \end{aligned} \quad (5)$$

Following this, it also can be expressed as

$$\begin{aligned} \min_{w_l, t_l} \sum_{l=1}^d \|x_l * t_l - y\|^2 + \lambda \|w_l\|^2 \\ \text{s.t. } t_l = c \odot w_l \end{aligned} \quad (6)$$

Note that, in the special case where $\text{diag}(c)$ is invertible, Eq.5 can be written

$$\min_{t_l} \sum_{l=1}^d \|X_l^\top t_l - y\|_2^2 + \lambda \|\text{diag}(c)^{-1}t_l\|_2^2 \quad (7)$$

It is easy to see that Eq.7 is equivalent to SRDCF [7].

3.2 Online Optimization

To solve the optimization problem Eq.6, we apply the augmented Lagrangian [27] used in [26]. First, by applying Parseval's theorem to Eq.6, the filter w can be equivalently computed in the Fourier domain by minimizing the following loss function with the constraint,

$$\begin{aligned} \min_{\hat{w}_l, \hat{t}_l} \sum_{l=1}^d \|\hat{x}_l \odot \hat{t}_l - \hat{y}\|^2 + \lambda \|w_l\|^2 \\ \text{s.t. } \hat{t}_l = \widehat{c \odot w_l} \end{aligned} \quad (8)$$

Then, by introducing augmented Lagrange multipliers to incorporate the equality function into the loss function, the Lagrangian function is formulated as,

$$\begin{aligned} L(\hat{t}_l, w_l, \hat{\zeta}_l) \\ = \sum_{l=1}^d \|\text{diag}(\hat{x}_l)\hat{t}_l - \hat{y}\|^2 + \lambda \|w_l\|^2 + [\hat{\zeta}_l^\top (\hat{t}_l - \widehat{c \odot w_l}) \\ + \widehat{\hat{\zeta}_l^\top (\hat{t}_l - \widehat{c \odot w_l})}] + \mu_l \|\hat{t}_l - \widehat{c \odot w_l}\|^2, \end{aligned} \quad (9)$$

where $\hat{\zeta}_l$ is the Fourier transformation of the Lagrange multipliers and μ_l denotes penalty parameter which controls the rate of convergence. The optimization problem Eq.4 is transformed to minimize the Lagrangian function with the variables \hat{t}_l, w_l and the Lagrange multipliers $\hat{\zeta}_l, \mu_l$. It can be optimized by iteratively solving some subproblems with closed form solutions. When a subproblem is solved for a variable, the other variables with their recent values are fixed. Thus Eq.9 can be solved by sequentially iterating the following three steps.

Updating \hat{t}_l : Given the others, the minimization problem Eq.9 for $\{\hat{t}_l\}_{l=1}^d$ can be decomposed into d independent subproblems. The l -th subproblem is solved as,

$$\begin{aligned} \hat{t}_l = \underset{\hat{t}_l}{\text{argmin}} \|\text{diag}(\hat{x}_l)\hat{t}_l - \hat{y}\|^2 + [\hat{\zeta}_l^\top (\hat{t}_l - \widehat{c \odot w_l}) \\ + \widehat{\hat{\zeta}_l^\top (\hat{t}_l - \widehat{c \odot w_l})}] + \mu_l \|\hat{t}_l - \widehat{c \odot w_l}\|^2 \\ = \frac{\widehat{\hat{x}_l \odot \hat{y}} - \hat{\zeta}_l + \mu_l \widehat{c \odot w_l}}{\widehat{\hat{x}_l \odot \hat{x}_l} + \mu_l} \end{aligned} \quad (10)$$

where \div denotes the element-wise division and $\widehat{\hat{x}_l}$ indicates the complex-conjugate of \hat{x}_l .

Updating w_l : Given the others, the minimization problem Eq.9 for $\{w_l\}_{l=1}^d$ can be decomposed into d independent subproblems. The l -th subproblem is solved as,

$$\begin{aligned} w_l = \underset{w_l}{\text{argmin}} \lambda \|w_l\|^2 + [\hat{\zeta}_l^\top (\hat{t}_l - \widehat{c \odot w_l}) \\ + \widehat{\hat{\zeta}_l^\top (\hat{t}_l - \widehat{c \odot w_l})}] + \mu_l \|\hat{t}_l - \widehat{c \odot w_l}\|^2 \\ = \frac{c \odot \mathcal{F}^{-1}(\hat{\zeta}_l + \mu_l \hat{t}_l)}{\lambda + \mu_l c \odot c} \end{aligned} \quad (11)$$

where \div denotes the element-wise division.

Updating Multiplier $\hat{\zeta}_l$: We update the Lagrange multipliers as,

$$\hat{\zeta}_l \leftarrow \hat{\zeta}_l + \mu_l (\hat{t}_l - \widehat{c \odot w_l}) \quad (12)$$

$$\mu_l = \min(\mu_{max}, \beta \mu_l) \quad (13)$$

In experiment, we set $\mu_1 = \dots = \mu_l = \dots = \mu_d = \mu$.

The full derivation is presented in the supplementary material.

3.3 Model Update Strategy

In visual tracking, the linear interpolation is widely used. Here, we more deeply investigate the linear interpolation during the tracking.

The filter w^k used for the next $k + 1$ frame can be reformulated as

$$\begin{aligned} w^k = & (\varrho - \alpha)^{k-1} w_*^1 + (\varrho - \alpha)^{k-2} \alpha w_*^2 \\ & + \dots + (\varrho - \alpha) \alpha w_*^{k-1} + \alpha w_*^k \end{aligned} \quad (14)$$

where w_*^k is the filter which is obtained from the k th frame and ϱ is the sum of the update rates every frame. When k is less than $\log_{\varrho-\alpha} \alpha$, the weight of w_*^1 is greater than the weight of w_*^k . An inaccurate tracking results easily causes a deterministic failure when the target is severely occluded, in the beginning of tracking. Only, w_*^1 is absolutely accurate. To strengthen the robustness, we increase the weight proportion of the w_*^1 by making ϱ greater. But note that keep $\varrho - \alpha < 1$. For example, when the learning rate α is conventionally set to 0.02, set ϱ to 1.01.

3.4 Our Tracking Framework

The tracking for an image sequence is mainly as follows including training, detecting.

Training: For the standard CF, there are IRs in training samples from cyclic shifts of a base training sample. Therefore, we introduce a spatial map to filter the training samples within the standard CF formulation. New training samples are needed to be extracted and a new model should be trained for predicting in the next frame, when the object is located in the current frame of the image sequence. According to Eq.4, we train a new model by a new base training sample x_t . The new base training sample is centered at the object location, and its scope is approximately four times as big as the target's. Here, t is the number of the current frame.

Detecting: In the detection stage, the tracker estimates the target location as a new frame comes. Centered at the target location in previous frame, a base detecting sample z is extracted from the new frame. For the base detecting sample z , we compute the response S as,

$$S(z) = \mathcal{F}^{-1} \left(\sum_{l=1}^d \hat{z}_l \odot \widehat{w_l \odot c} \right), \quad (15)$$

The location with the maximum in the response is about the translation. And we apply the sub-grid interpolation strategy [7] to maximize the scores of the response. Meanwhile, multiple base training samples with different sizes centered around the target are used for estimating the target scale. Let $M \times N$ denote the fiducial search size and κ be the current change factor of the target. The size of a base training sample x_{a^r} is $M\kappa a^r \times N\kappa a^r$. Here, a is the scale increment factor, $r \in \{\lfloor \frac{1-s}{2} \rfloor, \dots, \lfloor \frac{s-1}{2} \rfloor\}$ and s denotes the number of scales. A base training sample x_{a^r} is resized to the fiducial search size before the model computation. The current change factor of the target κ is updated according to scale change, as the target is located in the frame.

An overview of our tracker is summarized in Algorithm 1.

Algorithm 1 RFCT algorithm

Require: Frame sequence $\{I\}_{k=1}^K$, the initial location b_1 , desired response y , spatial map c

Ensure: Tracking result for each frame b_k

- 1: **repeat**
 - 2: Crop several search regions with different scales from the frame I_k , which are centered at the last location b_{k-1} , and extract features of each region z_r .
 - 3: Calculate the response of each base sample z_r using Eq.15 to estimate the location and scale of the target.
 - 4: **while** stop condition **do**
 - 5: Update \hat{t}_l using Eq.10
 - 6: Update w_l using Eq.11
 - 7: Update $\hat{\zeta}_l, \mu_l$ using Eq.12 and Eq.13
 - 8: **end while**
 - 9: Update the filter by the linear interpolation.
 - 10: **until** the end of the sequence
-

4 Experiment Results

In this section, we first present the experimental setup. Then, we analyse the effects of three spatial maps and the increasing of the weights for accurate filters. Finally, we compare the proposed method with trackers based on conventional features and trackers based on deep features respectively.

4.1 Experimental Setup

Here, we present experimental setup, datasets and evaluation metrics.

Parameters Setup: Similar to [1,26,2], we apply HOG and Color-Names features multiplied by a Hann window for the filter w . A cell size of 4×4 pixels is employed for HOG features, and the image region area of a base training sample is 4^2 times the target size. The label y is a Gaussian map with a standard deviation proportional to the target size. The sum of update rates is set to 1.01, and the learning rate is set to 0.02. The augmented Lagrangian optimization parameters are set to $\mu^{(0)} = 5$, $\beta = 3$ and $\mu_{max} = 20$.

In addition, we set the number of iterations is 8.

Datasets: We evaluate the proposed tracker on two datasets: OTB-2013 [28] and OTB-2015 [29]. There are 50 videos annotated with ground truth bounding boxes and various visual attributes in OTB-2013. The recently introduced OTB-2015 is an expansion of OTB-2013, containing 100 sequences.

Evaluation Metrics: The proposed method is compared with state-of-the-art trackers, employing the evaluation metrics and code provided by the benchmark datasets. Our approach is quantitatively evaluated in two aspects in [28], precision rate and success rate. Distance precise (DP) is widely used for precision rate, the percentage of frames whose distance between the center locations of the tracked targets and the manually labeled ground truths is within a given threshold distance of the ground truth. The threshold is commonly set to 20 pixels. Overlap precise (OP) is applied for success rate, the ratios of successful frames whose overlap between the tracked bounding box and the ground truth bounding box is larger than a given threshold. The threshold is varied from 0 to 1. The specific threshold 0.5 and the area under curve (AUC) of a success plot are usually used to rank the tracking algorithms respectively.

4.2 Analysis of RFCT

The values of the spatial map are not restricted in our proposed method. Therefore, we demonstrate the effects of three spatial maps by experiments on OTB-2013. When none of the values in the spatial map is zero, our proposed Eq.7 is equivalent to SRDCF [7]. Therefore, the quadratic function in SRDCF is chose to design a spatial map $c(p, q) = [\nu + \delta(p/W)^2 + \delta(q/H)^2]^{-1}$, which is named Rquadratic Map. Here, $W \times H$ is the target size. We aims to eliminate the interference of the IR. At the same time, considering severe deformation, the surrounding nearly around the target may bring the discriminative information. We alter the above Rquadratic Map, setting the values beyond the region with 1.6 times the target region to zero. The altered map is named Our Map. In addition, we take a binary map with 1 in the target region and 0 in the other region for comparison, named Binary Map. The tracking results based on the above three maps are summarized in Table 1.

As the shown in Table 1, Our Map is a little better than the other two maps. Further, based on Our Map, we implement a tracker named RFCT increasing the weight proportions of accurate filters. In Table 1, the result clearly shows that the increase brings the positive effect.

Table 1. Analysis of our approach on OTB-2013. We report the area-under-the-curve (AUC) scores (%). The **first** and **second** rank values are highlighted in color.

	Our trackers based on different maps			RFCT
	Binary Map	Rquadratic Map	Our Map	
OTB-2013	58.0	61.5	62.6	65.9

4.3 Comparison with Trackers based on Conventional Features

We evaluate the proposed method on the benchmark OTB-2013 and OTB-2015 with comparisons to 42 trackers using conventional hand-crafted features, including 41 trackers in [28], and these state-of-the-art trackers ECO-HC [1], BACF [3], SRDCFdecon [30], CSR-DCF [26], STAPLE_{CA} [4], SRDCF [7], CFBL [8], LCT [31], SAMF [12], MEEM [32], DSST [16] and KCF [6].

Table 2. Success rates (%) of RFCT compared with these conventional features based trackers mentioned above at an overlap threshold 0.5. For clarity, only the top 10 trackers are displayed. The top 3 rank values are highlighted by red, green and blue respectively.

	RFCT	ECO-HC [1]	SRDCFdecon [30]	BACF [3]	CSR-DCF [26]	STAPLE _{CA} [4]	SRDCF [7]	LCT [31]	SAMF [12]	MEEM [32]
OTB-2013	84.1	81.0	81.4	84.0	75.6	76.5	78.1	81.3	73.2	69.6
OTB-2015	77.2	78.4	76.6	77.6	70.8	72.8	72.9	70.1	67.5	62.2

Table 2 reports the success evaluation of our method and those conventional trackers at an overlap threshold 0.5. For the sake of clarity, we present the top 10 trackers in the table. Among these trackers, ECO-HC and BACF perform better results with an overlap precise of 81.0%, 84% on OTB-2013 and an overlap precise of 78.4%, 77.6% on OTB-2015 respectively. The proposed RFCT performs well with an overlap precise of 84.1% on OTB-2013 and an overlap precise of 77.2% on OTB-2015. The results show that our method achieves comparable results as ECO-HC. Our RFCT performs well than other trackers, the details are as followed. (1) Among these conventional correlation filter tracking algorithms apart from the BACF and ECO-HC, SRDCFdecon and SRDCF are 2 top existing trackers. On OTB-2013, SRDCFdecon and SRDCF achieve OP of 81.4%, 78.1% respectively. Our approach generates better tracking results by 2.7% and 6%. On OTB-2015, SRDCFdecon and SRDCF separately achieve OP of 76.6%, 72.8%. Our method performs slightly better tracking results by 0.6% and 4.4%. (2) Compared with these trackers except correlation filter tracking algorithms, the proposed method achieve better tracking performance against MEEM the best tracker by 14.5% on OTB-2013 and 15.0% on OTB-2015.

Fig. 3 compares RFCT with these conventional tracking algorithms, containing precision and success plots illustrating distance precise (DP) and overlap precise (OP) on OTB-2013 and OTB-2015. For success plots, AUCs are reported in brackets. In both precision and success plots on OTB-2013, the proposed RFCT approach achieves slightly better performance. On OTB-2015, our tracker shows comparable results as BACF, SRDCFdecon and outperforms other trackers. These results demonstrate the importance of filtering training samples to learn a more robust tracker. This evaluation also shows that the proposed method is effective.

Attribute Based Comparison: We show an attribute based evaluation of the proposed approach on OTB-2013. The dataset videos are annotated with 11 different attributes namely occlusion, deformation, motion blur, fast motion, in-plane rotation, out-of-plane

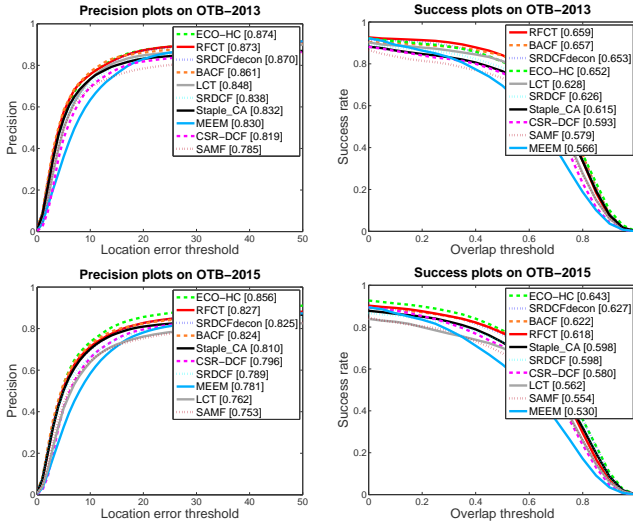


Fig. 3. Precision and success plots reporting a comparison with the conventional features based trackers on OTB-2013 and OTB-2015 datasets. For clarity, we only present the top 10 trackers in each plot. The area-under-the-curve (AUC) score of each tracker is reported in a bracket for success plots.

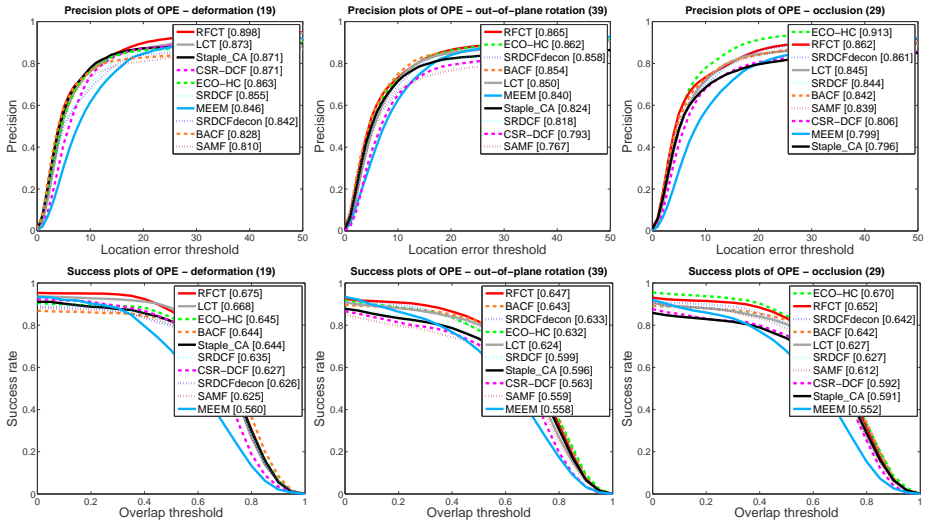


Fig. 4. Attribute based evaluation. Precision and success plots compare the proposed RFCT method with these conventional features based trackers over four tracking challenges on OTB-2013. AUCs are reported in brackets for success plots. For clarity, only the top 10 trackers are showed in each plot.

rotation, illumination, out-of-view, variation, background clutter, and low resolution. A tracker can be analysed in the 11 different aspects. Due to space constraints, we present precision and success plots of OPE for 4 attributes in Fig. 4 and more results can be found in the supplementary material. And for clarity, only the top 10 trackers are showed in each plot. In cases of deformation and out-of-plane rotation, the proposed algorithm performs well against other trackers. In case of occlusion, our tracker shows better results than SRDCFdecon.

Robustness to Initialization: We evaluate the robustness of our approach to different temporal and spatial initialization on OTB-2013 using two metrics [28], spatial robustness evaluation (SRE) and temporal robustness evaluation (TRE). SRE evaluate the sensitivity of a tracker when initialize the tracker by different bounding boxes. TRE shows the performance of a tracker with different initializations at different start frames in a video. Fig. 5 shows the SRE and TRE success plots of RFCT with these conventional feature base trackers mentioned above on OTB-2013. The proposed RFCT tracker achieves comparable AUC scores as ECO-HC and BACF, and performs well against other trackers.

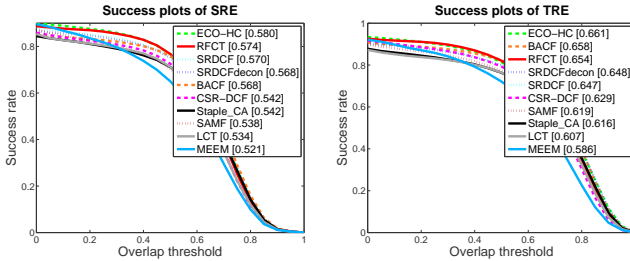


Fig. 5. Robustness based evaluation. The success plots on SRE and TRE compare RFCT with these above trackers based on conventional features based on OTB-2013. AUCs are reported in brackets, and only the top 10 trackers are showed in each plot for clarity.

4.4 Comparison with Correlation Trackers based on Deep Features

We also compare the proposed approach based on conventional features with the several state-of-the-art trackers based deep features including MCPF [33], DeepSRDCF [34], HDT [35] on OTB-2013 and OTB-2015 dataset.

Table 3 shows success rates of the conventional features based RFCT tracker compared with the several deep feature based trackers at an overlap threshold 0.5. Among the existing methods, MCPF performs best with the AUC scores of 85.8% on OTB-2013 and 78.0% on OTB-2015. Our approach achieves the AUC scores of 84.1% on OTB-2013 and 77.2% on OTB-2015. The proposed method shows comparable results as MCPF. And our approach slightly outperforms DeepSRDCF and HDT on the both datasets.

Fig. 6 compares the proposed method based on conventional features with the several deep features based trackers on OTB-2013 and OTB-2015, showing the DP for precision plot and AUC score for success plot of each tracking algorithm. Overall, MCPF performs better among the existing methods. For AUC score, it achieves a gain of 1.8% on OTB-2013 and 1.0% on OTB-2015 compared to our approach. Note that, our approach is based on conventional features.

Table 3. Success rate (%) of RFCT compared to the above trackers based on deep features at an overlap threshold 0.5. The **first**, **second** and **third** rank values are highlighted in color.

	RFCT	DeepSRDCF [34]	HDT [35]	MCPF [33]
OTB-2013	84.1	79.4	73.7	85.8
OTB-2015	77.2	77.2	65.8	78.0

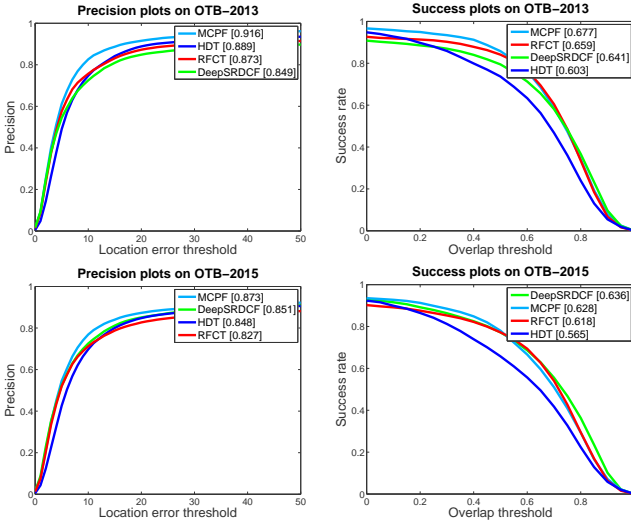


Fig. 6. Precision and success plots of RFCT compared with the deep features based trackers on OTB-2013 and OTB-2015 datasets. The AUC score of each tracker is displayed in a bracket for success plots.

5 Conclusion

In this paper, we propose Region-filtering Correlation Tracking (RFCT) to learn a robust filter for visual tracking. Compared with current CF trackers, the proposed RFCT

method filters training samples to focus on more interesting region in training samples by a spatial map. It is a more general way to control background information and target information in training samples. By comparison, Our Map is better than the other two maps in experiments. Moreover, we increase the weight proportions of accurate filters to alleviate model corruption during tracking. Quantitative evaluations on OTB-2013 and OTB-2015 benchmark datasets demonstrate that the proposed RFCT tracking algorithm performs well against several state-of-the-art trackers.

References

1. Danelljan, M., Bhat, G., Khan, F.S., Felsberg, M.: Eco: Efficient convolution operators for tracking. *Proceedings of the IEEE Conference on Computer Vision and Pattern Recognition* (2017)
2. Danelljan, M., Robinson, A., Khan, F.S., Felsberg, M.: Beyond correlation filters: Learning continuous convolution operators for visual tracking. In: *Proceedings of European Conference on Computer Vision*. (2016) 472–488
3. Kiani Galoogahi, H., Fagg, A., Lucey, S.: Learning background-aware correlation filters for visual tracking. In: *Proceedings of the IEEE Conference on Computer Vision and Pattern Recognition*. (2017) 1135–1143
4. Mueller, M., Smith, N., Ghanem, B.: Context-aware correlation filter tracking. (2017)
5. Bolme, D.S., Beveridge, J.R., Draper, B.A., Lui, Y.M.: Visual object tracking using adaptive correlation filters. In: *Proceedings of the IEEE Conference on Computer Vision and Pattern Recognition*, IEEE (2010) 2544–2550
6. Henriques, J.F., Caseiro, R., Martins, P., Batista, J.: High-speed tracking with kernelized correlation filters. *IEEE Transactions on Pattern Analysis and Machine Intelligence* **37**(3) (2015) 583–596
7. Danelljan, M., Hager, G., Shahbaz Khan, F., Felsberg, M.: Learning spatially regularized correlation filters for visual tracking. In: *Proceedings of the IEEE International Conference on Computer Vision*. (2015) 4310–4318
8. Kiani Galoogahi, H., Sim, T., Lucey, S.: Correlation filters with limited boundaries. In: *Proceedings of the IEEE Conference on Computer Vision and Pattern Recognition*. (2015) 4630–4638
9. Kiani Galoogahi, H., Sim, T., Lucey, S.: Multi-channel correlation filters. In: *Proceedings of the IEEE International Conference on Computer Vision*. (2013) 3072–3079
10. Danelljan, M., Shahbaz Khan, F., Felsberg, M., Van de Weijer, J.: Adaptive color attributes for real-time visual tracking. In: *Proceedings of the IEEE Conference on Computer Vision and Pattern Recognition*. (2014) 1090–1097
11. Danelljan, M., Häger, G., Khan, F.S., Felsberg, M.: Coloring channel representations for visual tracking. In: *Proceedings of Scandinavian Conference on Image Analysis*. (2015) 117–129
12. Li, Y., Zhu, J.: A scale adaptive kernel correlation filter tracker with feature integration. In: *Proceedings of European Conference on Computer Vision Workshops*. (2014) 254–265
13. Tang, M., Feng, J.: Multi-kernel correlation filter for visual tracking. In: *Proceedings of the IEEE International Conference on Computer Vision*. (2015) 3038–3046
14. Dalal, N., Triggs, B.: Histograms of oriented gradients for human detection. In: *Proceedings of the IEEE Computer Society Conference on Computer Vision and Pattern Recognition*. Volume 1. (2005) 886–893
15. Van De Weijer, J., Schmid, C., Verbeek, J., Larlus, D.: Learning color names for real-world applications. *IEEE Transactions on Image Processing* **18**(7) (2009) 1512–1523

16. Danelljan, M., Häger, G., Khan, F., Felsberg, M.: Accurate scale estimation for robust visual tracking. In: Proceedings of British Machine Vision Conference. (2014)
17. Bibi, A., Mueller, M., Ghanem, B.: Target response adaptation for correlation filter tracking. In: Proceedings of European Conference on Computer Vision. (2016) 419–433
18. Wang, M., Liu, Y., Huang, Z.: Large margin object tracking with circulant feature maps. Proceedings of the IEEE Conference on Computer Vision and Pattern Recognition (2017)
19. Hare, S., Golodetz, S., Saffari, A., Vineet, V., Cheng, M.M., Hicks, S.L., Torr, P.H.: Struck: Structured output tracking with kernels. IEEE transactions on pattern analysis and machine intelligence **38**(10) (2016) 2096–2109
20. Sui, Y., Zhang, Z., Wang, G., Tang, Y., Zhang, L.: Real-time visual tracking: Promoting the robustness of correlation filter learning. In: Proceedings of European Conference on Computer Vision. (2016) 662–678
21. Liu, S., Zhang, T., Cao, X., Xu, C.: Structural correlation filter for robust visual tracking. In: Proceedings of the IEEE Conference on Computer Vision and Pattern Recognition. (2016) 4312–4320
22. Li, Y., Zhu, J., Hoi, S.C.: Reliable patch trackers: Robust visual tracking by exploiting reliable patches. In: Proceedings of the IEEE Conference on Computer Vision and Pattern Recognition. (2015) 353–361
23. Liu, T., Wang, G., Yang, Q.: Real-time part-based visual tracking via adaptive correlation filters. In: Proceedings of the IEEE Conference on Computer Vision and Pattern Recognition. (2015) 4902–4912
24. Zuo, W., Wu, X., Lin, L., Zhang, L., Yang, M.H.: Learning support correlation filters for visual tracking. arXiv preprint arXiv:1601.06032 (2016)
25. Zhang, T., Bibi, A., Ghanem, B.: In defense of sparse tracking: Circulant sparse tracker. In: Proceedings of the IEEE Conference on Computer Vision and Pattern Recognition. (2016) 3880–3888
26. Lukežič, A., Vojšíř, T., Čehovin, L., Matas, J., Kristan, M.: Discriminative correlation filter with channel and spatial reliability. Proceedings of the IEEE Conference on Computer Vision and Pattern Recognition (2017)
27. Boyd, S., Parikh, N., Chu, E., Peleato, B., Eckstein, J.: Distributed optimization and statistical learning via the alternating direction method of multipliers. Foundations and Trends® in Machine Learning **3**(1) (2011) 1–122
28. Wu, Y., Lim, J., Yang, M.H.: Online object tracking: A benchmark. In: Proceedings of the IEEE conference on computer vision and pattern recognition. (2013) 2411–2418
29. Wu, Y., Lim, J., Yang, M.H.: Object tracking benchmark. IEEE Transactions on Pattern Analysis and Machine Intelligence **37**(9) (2015) 1834–1848
30. Danelljan, M., Hager, G., Shahbaz Khan, F., Felsberg, M.: Adaptive decontamination of the training set: A unified formulation for discriminative visual tracking. In: Proceedings of the IEEE Conference on Computer Vision and Pattern Recognition. (2016) 1430–1438
31. Ma, C., Yang, X., Zhang, C., Yang, M.H.: Long-term correlation tracking. In: Proceedings of the IEEE Conference on Computer Vision and Pattern Recognition. (2015) 5388–5396
32. Zhang, J., Ma, S., Sclaroff, S.: Meem: robust tracking via multiple experts using entropy minimization. In: Proceedings of European Conference on Computer Vision. (2014) 188–203
33. Zhang, T., Xu, C., Yang, M.H.: Multi-task correlation particle filter for robust object tracking. In: Proceedings of IEEE Conference on Computer Vision and Pattern Recognition. Volume 7. (2017)
34. Danelljan, M., Hager, G., Shahbaz Khan, F., Felsberg, M.: Convolutional features for correlation filter based visual tracking. In: Proceedings of the IEEE International Conference on Computer Vision Workshops. (2015) 58–66

35. Qi, Y., Zhang, S., Qin, L., Yao, H., Huang, Q., Lim, J., Yang, M.H.: Hedged deep tracking. In: Proceedings of the IEEE Conference on Computer Vision and Pattern Recognition. (2016) 4303–4311